2010 IEEE International Conference on Robotics and Automation
Anchorage Convention District
May 3-8, 2010, Anchorage, Alaska, USA

Design and Evaluation of a Fin-Based Underwater Propulsion System

Benjamin Peter, Roman Ratnaweera, Wolfgang Fischer, Dr. C. Pradalier and Prof. Dr. R. Y. Siegwart
Autonomous Systems Lab, ETH Zürich, Zürich, Switzerland

***Abstract*— In search of underwater locomotion methods as alternatives to propellers, systems relying on the propagation of waves along a fin have already been designed and evaluated by several scientists. Considerable effort has been undertaken to optimise their efficiency both by fluid dynamic analysis and experiments on physical prototypes. One drawback of the systems hitherto has been their electro-mechanical complexity in that they required many actuators and refined control strategies to generate the desired fin undulation. Our approach has been to translate the result of these optimisations into a simpler, purely mechanical model relying on the principle of camshafts to achieve a similar undulatory fin motion. The goal was to evaluate whether this type of propulsion system is feasible and whether it was a viable alternative to propellers in Autonomous Underwater Vehicles. The prototype built during the project, CUTTLEFIN, reached comparable speeds to other undulating robot solutions. Force measurements also showed that the thrust produced is in qualitative accordance to a simplified fluid dynamics model. This makes the camshaft approach a promising option for generating an undulating wave in a membrane-based fin propulsion system, if one is willing to pay the price of lower flexibility compared to current dexterously actuated solutions.**

I. INTRODUCTION

Even though robotics will never achieve the same level of elegance and perfection as nature, insight can be gained by looking at biological systems for inspiration. The dream of this line of projects is to design an Autonomous Underwater Vehicle (AUV) for long term data harvesting in environments such as coral reefs. Figure 1 sketches a rough idea of how the shell of a turtle could be combined with the locomotion concept found in cuttlefish. The first step of this project was to evaluate this type of propulsion and analyse if it was applicable to the task.

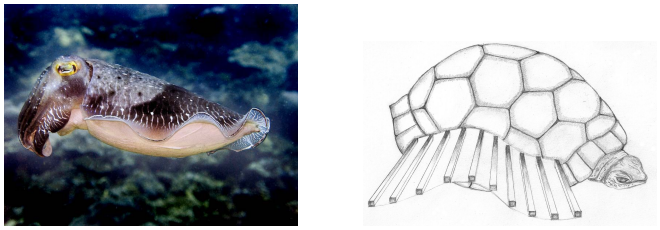

1: Inspiration and design idea for propulsion of a turtle-like AUV (M. Svoboda)

A. Motivation

According to scientists such as K.H. Low [1] [2] and M. Sfakiotakis [3], there is a demand for efficient underwater propulsion systems that exhibit high manoeuvrability and dexterous manipulation. The principle of undulation presents a promising candidate for these demands. For military applications, noiseless propulsion and an inconspicuous wake would be additional incentives. Our reasons for seeking alternate methods of propulsion to propellers were threefold. One, according to our prior experience with AUVs, propellers are prone to entanglement in rich marine environment (algae and wires) and a more robust system in this respect is desirable. Two, propellers are known to harm wildlife due to their noise emission (for example see [4]) and scarring whales. And three was the expectation of exploring something new.

Upon closer inspection it soon turned out that the field was not as novel as we believed. Analysis of the kinematics of undulating fin was conducted by Sir James Grey as early as the 1930s. With continued theoretical work as in [5], research has already produced some successful prototypes such as by Professor Low and others with efforts at optimisations in physical prototypes [6]. Building on this work, our approach has been a mechanical implementation relying on camshafts to generate the propagating wave. This brings about a dramatic reduction of necessary actuators compared to other undulatory robots. This simplification comes at the price of limited flexibility of parameter variation.

II. STATE OF THE ART

A. Biological Context

The most common way of generating thrust in fish is by propagating a backward-moving wave through their body and/or caudal fin, called BCF locomotion. Fewer species rely purely on what is called the median and/or pectoral fins (MPF) locomotion method to generate their forward thrust. Our inspirational example, the cuttlefish, is one member of this class. However many fish families, even those relying on BCF for propulsion, use MPF for manoeuvring and stabilisation [7]. An extreme example of manoeuvrability is the seahorse, studied in [8]. According to Breder and Edgerton, there are several factors that can be varied in the undulation to achieve this dexterity, among which are: interdistance, length and flexibility of fin rays and the amplitude, frequency and phase lag along the fin in time [3] [8]. The variations of these parameters allows the seahorse to precisely adjust the force components generated by its dorsal and anal fins.

Depending on which of the fins of a fish are responsible for thrust generation, the locomotion form is called amiiform, gymnotiform or rajiform, shown in figure 2.

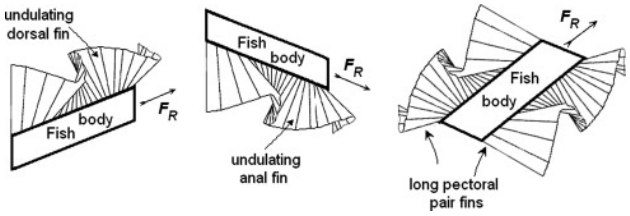

2: Amiiform, gymnotiform and rajiform fin undulations (Taken from [1])

B. Existing Underwater Robots

Several bio-inspired AUVs have already been built. Despite the fact that all of these robots aim to provide alternatives to propellers, their propulsion mechanisms differ substantially. For our project we focused on finding and analysing other robots that use fin undulation as primary method of propulsion. Some examples of AUVs using this kind of locomotion are:

- Cuttlefish robot, Nanyang Technological University [9]
- Knifefish robot, Northwestern University [6]

Note that all robots we encountered had a large number of actuators, most of them one actuator per ray. To avoid the resulting mechanical complexity, our objective was to implement fin undulation with only few actuators, preferably a single one.

III. Design Principle

A summary of the physical and behavioural parameters of fin undulations is shown in table I and visualised in figure 3. During the course of the project, solutions for different functions were evaluated, only one of which is shortly discussed in the next section.

I: Main parameters

Parameter		Description
Frequency	f	Frequency of the back-propagating wave
Amplitude	Θ	Maximum Amplitude of the fin wave
Number of rays	N	Number of rays
Waveform	$\theta_i(t)$	Angle of each ray i as a function of time
Phase delay	φ	Phase delay between two adjacent rays
Ray distance	d_{ray}	Distance between two adjacent rays
Wavelength	λ	Wavelength of the fin wave
Specific wavelength	w	Ratio of wavelength to total fin length
Fin length	L	Total length of the fin
Fin width	b	Width of the fin

Parameter relations:

- Fin length: $L = (N-1) \cdot d_{ray}$
- Wavelength: $\lambda = L \cdot \frac{1}{N-1} \frac{2\pi}{\varphi}$
- Specific wavelength: $w = \frac{\lambda}{L}$

A. Joint closure

Joint closure is one design decision that had an impact on the possible parameter variations and thereby the comparison to the mathematical model which is discussed later. Therefore the four options from figure 4 are shortly introduced.

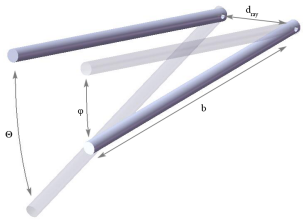

3: Problem parameter visualisation. Maximum deflection amplitude Θ, phase delay between rays φ, distance between rays d_{ray} and fin width b.

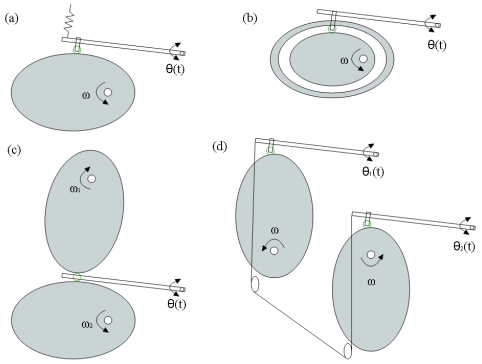

4: Joint closure options 1 to 4 of section III-A

1) Spring system (force closure): the follower is pressed on the cam by a spring; rejected due to excessive friction losses.
2) Grooved cam (form closure): the follower is attached to the cam via a groove; rejected due to excessive manufacturing complexity.
3) Second cam disc (form closure): another cam disc presses the follower on the main cam disc; rejected to excessive mechanical complexity.
4) Cross coupling (force closure): two followers that are $180°$ phase-shifted relative to each other are coupled via a wire. The advantage of this approach was twofold. For one, we do not increase the friction as in (a) by applying additional normal force on the follower. At the same time, it can be implemented with comparatively small mechanical effort.

The final pulley and wire system is illustrated in fig. 5.

B. Parameter Decisions

Table II summarises the parameter decisions, taken on the basis of literature study and our experiences with a first prototype consisiting of only six rays. Their motivation is left out here for brevity.

C. Fluid Dynamics Model

To estimate the propulsive force of the fin, a simplified fluid dynamics model was implemented. The model is based on a basic equation calculating the drag force of a single propulsive element moving through a fluid [10]:

$$F = -\frac{1}{2}\rho C S \left|\left|v\right|\right|^2 u_v \tag{1}$$

Assembled fin

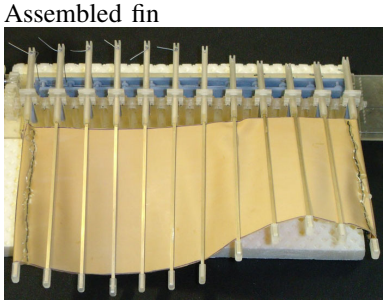

close-up on a single ray

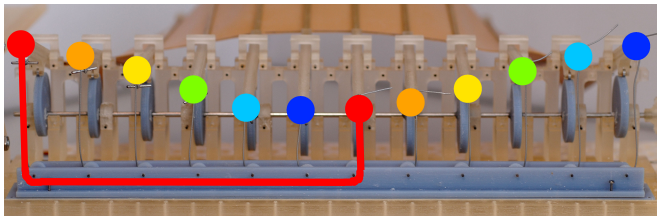

5: Pulley and wire system. The rear ends of each linked pair of rays which are 180° out of phase are marked by circles of the same colour. One wire is highlighted as an example.

II: Main parameter decisions

Parameter			Comment
Frequency	f	2Hz	Range around 2Hz according to [6]
Amplitude	Θ	15°	Range around 15° due to cam disc design
Number of rays	N	12	See specific wavelength, section III-D
Waveform	θ(t)	sine	Most often found in literature
Phase delay	φ	30°	See specific wavelength, section III-D
Ray distance	d_{ray}	$20mm$	Chosen due to overall dimension and waveform
Wavelength	λ	$240mm$	See section III-D
Specific wavelength	w	1.09	See section III-D
Fin length	L	$220mm$	Was a specification of the project
Fin width	b	$95mm$	Part of the fin design, see section III-E

where F is the force exerted by the fluid on the propulsive element, ρ is the density of the fluid, C is the drag coefficient, S is the effective area of the propulsive element, v is the velocity of the propulsive element and u_v is a unit vector in the direction of the velocity.

For a smooth, thin and flat body, the parallel force is negligible. Therefore, we can assume that the force acting normal to the surface of the propulsive element is nearly equal to the entire force on the element [10]:

$$F \cong F_\perp = -\frac{1}{2}\rho C S [v \cdot u_\perp]^2 u_\perp \tag{2}$$

where $F_\perp$ is the component of the drag force acting perpendicular to the surface of the propulsive element, v is the velocity relative to the fluid and $u_\perp$ is the unit vector normal to the surface of the element within 90° of the velocity vector.

To simplify the calculation of the propulsive force, the following assumptions were made:

- The mass of the rays and the fin are negligible
- The thickness of the rays and the fin are negligible
- All rays are rigid
- The fin is approximated by two triangles between each two rays. Each of these triangles is regarded as a flat plate moving through a fluid (figure 6).

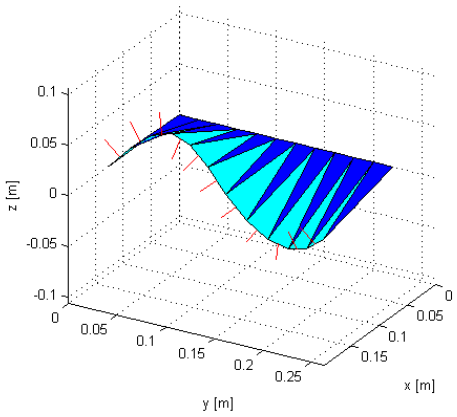

6: Fin approximated by triangles. The normal vectors are shown in red.

As an example, the expected forward thrust was $F_y = 111mN$ at our main operating point ($\Theta = 20°$, $f = 2$Hz, $w = 1.09$, $L = 220mm$, $L_{ray} = 115mm$, $N = 12$ rays). See section IV-C.3 for a comparison to measured values.

According to the optimisations of [6], the optimal specific wavelength for our model would have been 1.125. With the chosen joint closure (III-A), we were not able to choose arbitrary values for w as described in the next section. But $w = 1.09$ turned out to be reasonably close.

D. Specific Wavelength

The decision to use a wire coupling system limited the number of realisable phase delays and therefore specific wavelengths. All linked pairs of rays have to be 180° out of phase. This means that the phase delay can only be a whole fraction of 180°. Furthermore, the phase delay has to yield a value that guarantees that each ray has a complement. Therefore, the minimum value of the phase delay is $360°/N$, where N is the number of rays. Obviously, the number of rays has to be even.

The specific wavelength directly depends on the phase delay, as shown in equation 3:

$$w = \frac{360°}{\varphi} \cdot \frac{1}{N-1} \tag{3}$$

where w is the specific wavelength, φ is the phase delay and N is the number of rays. Using equation 3, the restrictions of the phase delay can be transferred to the specific wavelength. The table below shows the feasible phase delays and specific wavelengths for 12 rays:

Phase delay φ	specific wavelength w
180°	0.18
90°	0.36
60°	0.55
30°	1.09

The decision was to use 12 rays to have the flexibility to change the phase delay between two adjacent rays from $30°$ to $180°$. At a phase delay of $30°$, quite a smooth sine wave can be achieved. At a phase delay of $60°$, resulting in almost two full waves on the fin, the sine wave is still recognisable. When further increasing the phase delay, the waveform degenerates more and more to triangular shape.

E. Fin

Fish fins and undulation forms (figure 2) introduced in section II-A allow us to delineate the current solution used for evaluation purposes from the proposed final implementation in an AUV. The gymnotiform application served only as a test bench for measurements. The design idea from figure 1 calls for a rajiform configuration involving two of our proposed fins. Together with a pressure tank regulating the depth under water, we expect the system to be manoeuvrable in at least yaw, pitch, surge and heave directions.

If the rays in figure 5 provide the skeleton of the fin, it is the connecting membrane that makes the combination a fin capable of displacing water. Like other undulatory robots [2] [6], CUTTLEFIN employs a flexible elastomer for the reasons of flexibility and density. Natural rubber with a thickness of $0.5mm$ was chosen. Unlike in the quoted papers, the demand for elasticity was not very high since our rays allowed the material to slide through (see figure 5). The shape that the fin describes in space had to be projected onto a plane in order for the material to be cut. The required projection was calculated numerically by a summation of the distances of two rays. This is a function of time and of radial distance from the camshaft centre. Figure 7 shows the two shapes acquired by two different approximation methods used. In both cases, the goal was to best approximate the minimum occurring surface area of a full undulation. This way, there will always be a slight tension.

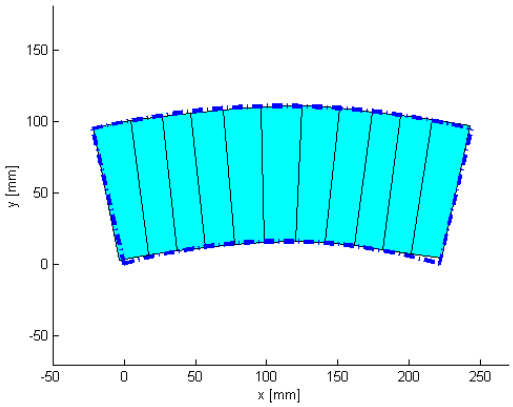

7: Fin shape approximations.

The density of the material is $1.01g/cm^3$, which is very desirable from the buoyancy point of view.

Based on observation of fish in nature, the ray is designed in such a way as to be flexible in the direction vertical to the fin and less so in axial direction. This was achieved by using thin brass profiles of 1x2 [mm].

F. Catamaran

To conduct tests and measurements with CUTTLEFIN, a polystyrene catamaran was built. The shape of this catamaran is one aspect that could be improved in a future attempt. Due to last-minute overloading of the catamaran, the waterline ended up higher than anticipated. The fluid dynamics of the test vehicle probably influenced the performance adversely by increasing the drag force on the catamaran.

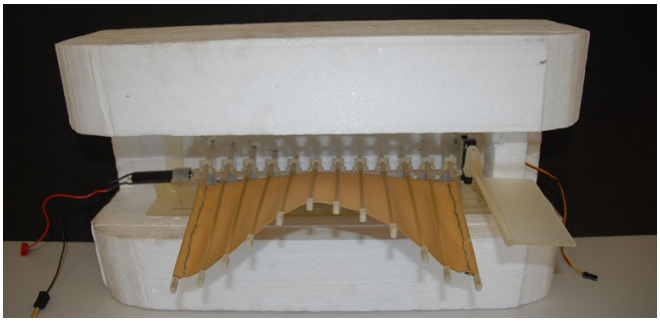

8: CUTTLEFIN attached to the catamaran.

IV. EVALUATION

The presented solution is evaluated based on measurements in a water channel and the simplified fluid dynamic model described in section III-C. The employed apparatus and the measurement approach is discussed before the presentation and discussion of the numerical results.

A. Apparatus

The water-towing tank at the Laboratory of Energy Conversion served as the testing environment. Its dimensions are 40x1x1 [m].

The forward thrust of the fin was measured using a spring balance suspended vertically, while a thin wire redirected the horizontal force around a bearing.

The voltage and the current were measured using standard multimeters mounted on the catamaran.

B. Measurement Procedure

This section shows which of the parameters from table II were varied to what extent, and how the values were recorded.

1) Parameter Variations: Since a change in the amplitude requires the complete removal of the camshaft, only three different amplitudes were examined, namely $\Theta = 10°$, $\Theta = 15°$ and $\Theta = 20°$. The maximum value was chosen due to mechanical constraints. Decreasing the amplitude further than $10°$ would result in a rapidly diminishing thrust, which would be hard to measure correctly.

For each value of the amplitude, the frequency was altered. With the throttle on the remote control, the frequency could be further adjusted. This was done at two settings: 100% and 75% or 50% throttle for each gear ratio.

The specific wavelength was kept at $w = 1.09$ at all times. An overview of the parameter variations can be found in the table below:

Parameter	Symbol	Range
Frequency	f	1Hz - 3Hz
Amplitude	Θ	10°, 15°, 20°
Specific wavelength	w	1.09

2) Measured Values: For each configuration, the following procedure was conducted at least twice: The catamaran was accelerated and then driven for 5 meters at constant speed, taking the time and counting the number of rotations. This allowed the calculation of the frequency f of the camshaft, as well as the speed v of the catamaran. To measure the actual electrical power consumption P of the motor, the current I flowing through the motor and the voltage V applied to the motor were monitored during the experiments. Second, the forward thrust F_y was measured by attaching the catamaran to the aforementioned spring balance apparatus. The thrust was then read from the spring balance displacement visually.

C. Results

1) Remarks: During the measurement process, some problems arose. The catamaran overload already mentioned (section III-F) and the approximation of the fin shape according to section III-E are examples. The approximation was only done for an amplitude of 20° due to consistency issues during the measurement process. Another problem was gear slippage, which occurred at certain configurations, especially at high frequencies. This can be explained by the suboptimal properties of the 3d-print material used for the spur gears.

2) Speed: The acquired speeds are displayed in figure 9. The differences in performance with $\Theta = 10°$,15° and 20° can clearly be seen. The maximum speed achieved was $26cm/s$ at $\Theta = 20°$ and $f = 2.3Hz$. This corresponds to approximately 1 fin length per second, which is a comparable result to that of rainbow trout with 1.2 body lengths per second at slow cruising speed [11]. It can be further noted that higher speeds would have been possible if no gear slippage had occurred (seen as crosses in figure 9).

3) Comparison to Fluid Dynamics Model: The obtained values of the forward thrust were compared to the fluid dynamics model described in section III-C. Examples for selected values are shown in the table below:

Amplitude Θ	Frequency f	Calculated Thrust F_y	Measured Thrust $F_y^{measured}$
10°	1.4Hz	11mN	65mN
15°	2.0Hz	59mN	265mN
20°	2.3Hz	147mN	407mN

The measured thrust exceeded the expected values calculated by the model. The discrepancy can in part be explained by the drastic simplifications of the model used, in part by the limitations of the measurement accuracy. Only the qualitative behaviour and the order of magnitude matched up.

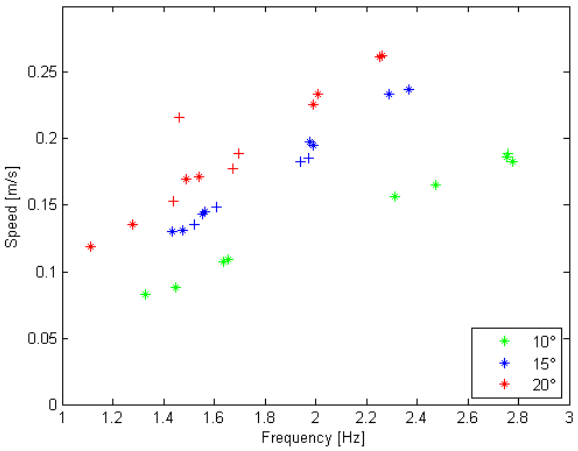

9: Speed of CUTTLEFIN. The asterisks represent the calculated values for the amplitudes $\Theta = 10°$,15° and 20°. Calculations using data where gear slipping occurred are displayed as crosses.

4) Efficiency: The Froude efficiency is defined as [12]:

$$\eta_F = \frac{P_E}{P_P} \tag{4}$$

where η_F is the Froude efficiency, P_E is the useful propulsive power and P_P is the time-averaged power expended by the prototype. η_F reflects the ability of the swimming body to impart useful kinetic energy to the water. This does not include friction losses in the mechanism itself, which have to be considered outside the Froude efficiency.

For steady state aquatic locomotion, high Reynolds numbers and a constant amplitude, the Froude efficiency only depends on the ratio between the speed of the backward wave travelling along the fin c and the forward speed u of the whole system. The Reynolds number of CUTTLEFIN is in the vicinity of $Re = 10^5$, which is high enough to use equation 5. For slender fish, the Froude efficiency can be calculated as follows [13]:

$$\eta_F = \frac{1}{2}\left(1 + \frac{u}{c}\right) \tag{5}$$

where u is the speed of the whole system (catamaran) and c is the speed of the backward wave on the fin.

Figure 10 shows the Froude efficiencies of the conducted measurements.

A Froude efficiency of about 65% to 80% compares to other results, for example the rainbow trout ($\eta_F = 74\%$) [11]. According to [12], the range for the Froude number of fish is from 90% for a carangiform swimmer to 16% for drag-based labriform locomotion.

However, the overall efficiency evaluated using the equation 6 leads to a maximum efficiency of only 2.6% at 20° amplitude.

$$\eta_{total} = \frac{u \cdot F_y}{I \cdot V} \tag{6}$$

where η_{total} is the overall efficiency coefficient, u is the velocity of the catamaran, F_y is the forward thrust, I is

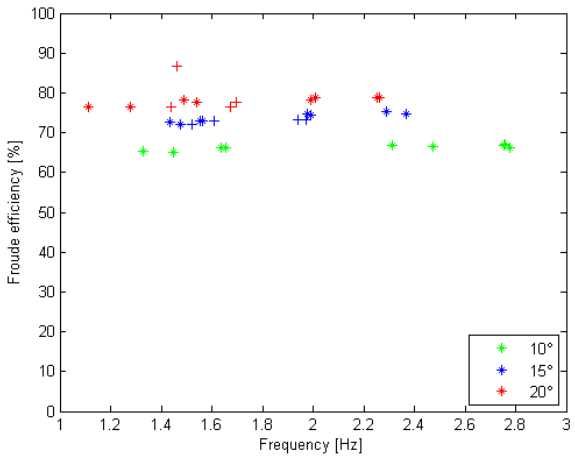

10: Froude efficiency of CUTTLEFIN. The asterisks represent the calculated values for the amplitudes $\Theta = 10°$,$15°$ and $20°$. Calculations using data where gear slipping occurred are displayed as crosses.

the electrical current flowing through the motor and V the voltage applied to the motor. It seems that from the electrical input power to kinetic power, we lose a factor of 40. Some of this can directly be accounted for in terms of known losses ($\eta_{motor,max} = 67\%$, $\eta_{planetary} = 60\%$, $\eta_{spurGear} \cong 90\%$) others would have to be analysed separately (friction losses in the camshaft approach, ill-suited form of catamaran etc). An implementation with realistic materials rather than 3D-print material would presumably introduce drastic improvements from a friction point of view.

V. CONCLUSION

Based on the performance of CUTTLEFIN, we conclude with an assessment of our work and propose directions for future work.

A. Assessment

The goal was to design and evaluate a locomotion concept for AUVs. The design and construction of the system required so much time that the evaluation was not as rigorous as would have been desirable. The results were highly satisfactory at first glance, but a more in-depth study of the performance would be recommendable if it is to be implemented in an AUV. Especially the question of manoeuvrability, which was not addressed in controlled experiments.

Nevertheless, CUTTLEFIN achieves comparable results in terms of speed and thrust to other undulatory systems with a minimum of necessary actuators. The mechanical realisation by means of a camshaft has on one hand the advantage that the propulsion system can be designed simple and robust. On the other hand, compared to other proposed robots, the solution is far less flexible in terms of the variety of generated waves.

It is the authors' belief that this type of locomotion is applicable to AUVs, at least at the scale of CUTTLEFIN. Scalability in both directions, smaller and larger, would have to be analysed separately. Whenever robustness of operation in marine flora and non-invasive coexistence with marine fauna is more important than speed or efficiency, propulsion through fin undulation is a promising alternative to the widely used propellers.

B. Future Work

CUTTLEFIN offers a wide and exciting spectrum of possible topics for follow-up projects with the end goal of designing an AUV using camshaft-generated fin undulation as means of propulsion. Some suggestions are:

- Rebuild CUTTLEFIN with better materials such as laser-cut cam discs and using exclusively non-corrosive metals to perform a more thorough and demanding evaluation of the performance
- Analyse the efficiency and compare it quantitatively to (a) other undulation-robots and (b) to other methods of propulsion such as propellers
- Investigate scalability of the fin
- Design an AUV hull while incorporating and water-sealing CUTTLEFIN
- Design, implement and test control strategies involving two fins and thus analyse manoeuvrability.

REFERENCES

[1] K. Low, "Modelling and parametric study of modular undulating fin rays for fish robots," *Mechanism and Machine Theory*, vol. 44, no. 3, pp. 615–632, 2009.

[2] A. Willy and K. Low, "Development and initial experiment of modular undulating fin for untethered biorobotic AUVs," in *2005 IEEE International Conference on Robotics and Biomimetics (ROBIO)*, 2005, pp. 45–50.

[3] M. Sfakiotakis, D. Lane, and J. Davies, "Review of fish swimming modes for aquatic locomotion," *IEEE Journal of Oceanic Engineering*, vol. 24, no. 2, pp. 237–252, 1999.

[4] Madsen, P., "How ships' traffic noise affects whales in a shipping channel," 2003, [Online; accessed April 2009].

[5] J. Lighthill and R. Blake, "Biofluiddynamics of balistiform and gymnotiform locomotion. Part 1. Biological background, and analysis by elongated-body theory," *Journal of Fluid Mechanics Digital Archive*, vol. 212, pp. 183–207, 2006.

[6] M. Epstein, J. Colgate, and M. MacIver, *Generating Thrust with a Biologically-inspired Robotic Ribbon Fin.* Northwestern University, 2006.

[7] J. Videler, *Fish swimming*. Chapman & Hall, 1993.

[8] C. Breder and H. Edgerton, "An analysis of the locomotion of the seahorse, hippocampus, by means of high speed cinematography*," *Annals of the New York Academy of Sciences*, vol. 43, no. 4 An Analysis of the Locomotion of the Seahorse, Hippocampus, by Means of High Speed Cinematography, pp. 145–172, 1942.

[9] K. Low, "Mechatronics and buoyancy implementation of robotic fish swimming with modular fin mechanisms," *Proceedings of the Institution of Mechanical Engineers, Part I: Journal of Systems and Control Engineering*, vol. 221, no. 3, pp. 295–309, 2007.

[10] M. Epstein, J. Colgate, and M. MacIver, "A biologically inspired robotic ribbon fin," in *Proceedings of IEEE/RSJ International Conference on Intelligent Robots and Systems*. Workshop on Morphology, Control, and Passive Dynamics, 2005.

[11] J. Nauen and G. Lauder, "Quantification of the wake of rainbow trout (Oncorhynchus mykiss) using three-dimensional stereoscopic digital particle image velocimetry," *Journal of Experimental Biology*, vol. 205, no. 21, pp. 3271–3279, 2002.

[12] J. Colgate and K. Lynch, "Mechanics and control of swimming: a review," *IEEE Journal of Oceanic Engineering*, vol. 29, no. 3, pp. 660–673, 2004.

[13] M. J. Lighthill, "Note on the swimming of slender fish," *Journal of Fluid Mechanics Digital Archive*, vol. 9, no. 02, pp. 305–317, 1960.